

Supplementary Materials

Screening of Additives to Ni-Based Methanation Catalyst for Enhanced Anti-Sintering Performance

Yuting Li ¹, Xiaoxia Han ², Chaofan Zhao ², Lin Yue ², Jinxian Zhao ¹ and Jun Ren ^{1,*}

¹ Key Laboratory of Coal Science and Technology, Taiyuan University of Technology, Ministry of Education and Shanxi Province, No. 79 Yingze West Street, Taiyuan 030024, China; liyuting0482@163.com (Y.L.); zhaojinxian@tyut.edu.cn (J.Z.)

² College of Electrical and Power Engineering, Taiyuan University of Technology, No. 79 Yingze West Street, Taiyuan 030024, China; hanxiaoxia@tyut.edu.cn (X.H.); fantasyzhao@foxmail.com (C.Z.); yuelin0282@link.tyut.edu.cn (L.Y.)

* Correspondence: renjun@tyut.edu.cn; Tel.: +86-351-6018598

Received: 20 April 2019; Accepted: 24 May 2019; Published: 28 May 2019

Contents1

Code

1. PCA dimensionality reduction code(R)

In our work, the number of input variables was reduced by PCA and the computer codes in this research were created by using the statistic language R:

```
> zz <- read.csv('data.csv')
> pca <- prcomp(zz[1:63, 1:16], scale = TRUE)
```

2. K-means clustering code(R)

Elements in the periodic table were categorized into seven groups by k-means clustering based on the six principal components, because a category containing only one member appeared if the categorization included eight or more groups. The R codes are listed below:

```
> z<-pca$x[1:63,1:6]
> y<-kmeans(z,7,nstart=3)
```

3. GPR model code(R)

Bgp in the **tpg** library for GPR developed by Gramacy was used for modeling. The R codes are listed below:

```
> library(tpg)
> pca <- read.csv('pcdata.csv', header=F)
> X <- pca[1:9,1:6]
> Z <- pca[1:9,7]
> XX <- pca[1:63,1:6]
> Symbol <- data.frame(symbol=pca[1:63,8])
> exp.bgp <- bgp(X = X, Z = Z, XX = XX, corr = "exp", improv = T, verb = 0)
```

Contents2

Explanation of the GPR model reliability

The optimization procedure, by means of GPR, will be explained using a simple example. Analysis was performed using statistical language R. The output was determined by a quadratic equation instead of a real experiment. The initial virtual experimental results are illustrated as “base” in Fig.1. The objective of this optimization is to determine the relationship between x and y of the figure. The first regression model was constructed using the five datasets and the **bgp** function. The output of the model was illustrated as a solid line in the figure, and the 90% confidence interval is presented as a dotted line. Experimental results (five datasets) were input to X and Z , additionally, an input grid for prediction were input to XX . The predictions are saved in variable ZZ .

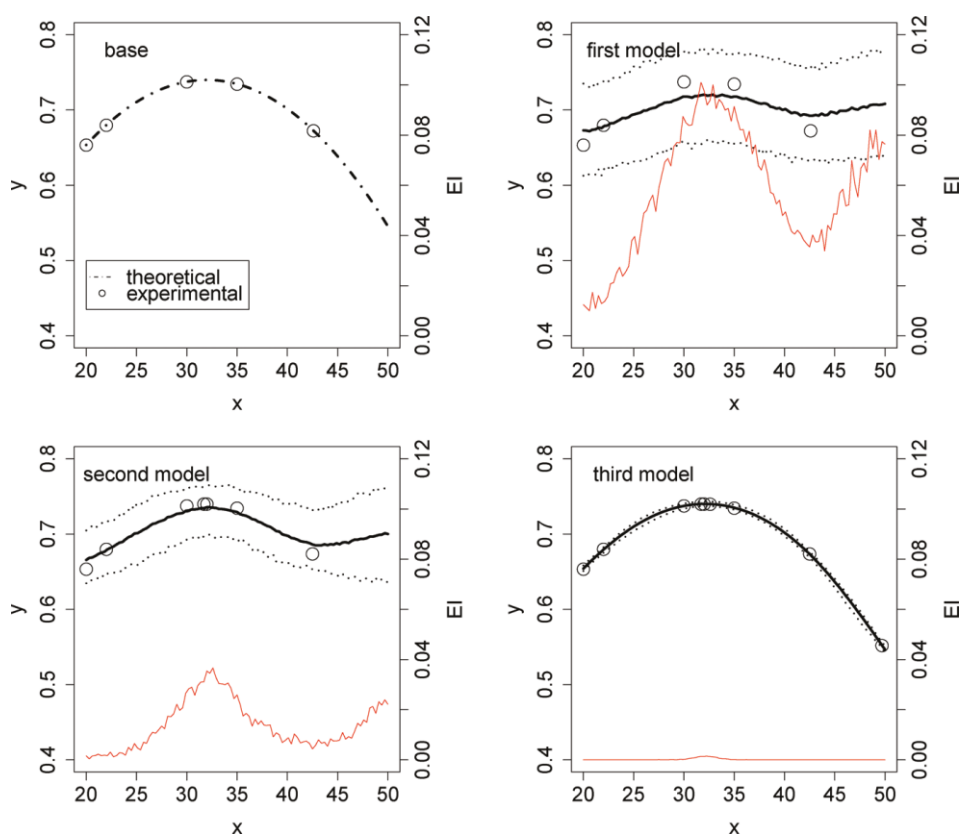


Figure S1 Model development by Gaussian process regression

```
> library(tgp)
> exp_x <- c(20, 22, 30, 35, 42.5)
> exp_y <- 0.74 - 6e-04 * (exp_x - 32) ^ 2
> th_x <- seq(20, 50, length = 101)
> first <- bgp(X = exp_x, Z = - exp_y, XX = th_x, corr = "exp", improv = c(1, 50), verb = 0)
> plot(exp_x, exp_y)
```

```
> lines(th_x, -first$ZZ.mean, lwd = 3)
> lines(th_x, -first$ZZ.q1, lty = 3, lwd = 2)
> lines(th_x, -first$ZZ.q2, lty = 3, lwd = 2)
> lines(th_x, first$improv$improv)
```

From the output of the first model, it is difficult to decide the maximum between the points at $x = 32$ and $x = 50$. Additional experiments are suggested by an index EI (expected improvement), as shown by the red line in the figure. EI shows the possible improvement of the accuracy and performance of the regression model after the experimental data is added to the model, and is a measure of the potential for new optima. EI was calculated from the **bgp** function, as shown below. In the first model, EI at $x = 31.7$ and $x = 32.0$ were the tops and these points were included in the second model. Thus, a total of seven datasets were used for the second regression model. The prediction, 90% confidence interval, and EI are illustrated as a second model in Fig.1. Using the additional experiments, the performance of the regression model was improved and the maxima were predicted correctly. However, the possibility remains that, in the figure, the maxima is located at $x = 50$. According to the suggestion by EI, two points ($x = 32.6, 49.7$) were included in the third model. As clearly shown in third model in Fig.1, the 90% confidence interval is quite narrow, and the maximum is predicted correctly. The solid line is almost same as the theoretical one. If the maximal EI becomes close to zero, as shown in the figure, the optimization procedure can be terminated because no further improvement is expected by conducting additional experiments.

We use this method to continuously improve the accuracy of the model. Gaussian process regression (GPR) has a good adaptability to dealing with complex problems such as high dimensionality, small sample, and nonlinearity. Its reliability has been proved by the paper[1-2]. Meanwhile, our experimental results also verify the reliability of this method. The predictions of W and Cs are slightly deviated, however, considering the estimation error, the prediction is not wrong and it is difficult to avoid for small dataset modeling.

[1] R.B. Gramacy, *tgp: An R Package for Bayesian Nonstationary, Semiparametric Nonlinear Regression and Design by Treed Gaussian Process Models*, Journal of Statistical Software, 19 (2007) 1-46.

[2] R.B. Gramacy, M. Taddy, Categorical Inputs, Sensitivity Analysis, Optimization and Importance Tempering with `tgp` Version 2, an R Package for Treed Gaussian Process Models, *Journal of Statistical Software*, 33 (2010) 1-48.

Contents3

Figure S2 XRD data of the CO methanation catalysts with 11 different additive elements before the reaction. (a) X-ray diffraction pattern with a diffraction angle between 10 and 80 degrees. (b) Partial enlargement of the characteristic peak of nickel (111) surface.

Figure S3 XRD data of the CO methanation catalysts with 11 different additive elements after the reaction. (a) X-ray diffraction pattern with a diffraction angle between 10 and 80 degrees. (b) Partial enlargement of the characteristic peak of nickel (111) surface.

Figure S4 XRD data of the CO methanation catalysts with 5 different additive elements before the reaction. (a) X-ray diffraction pattern with a diffraction angle between 10 and 80 degrees. (b) Partial enlargement of the characteristic peak of nickel (111) surface.

Figure S5 XRD data of the CO methanation catalysts with 5 different additive elements after the reaction. (a) X-ray diffraction pattern with a diffraction angle between 10 and 80 degrees. (b) Partial enlargement of the characteristic peak of nickel (111) surface.

Figure S2

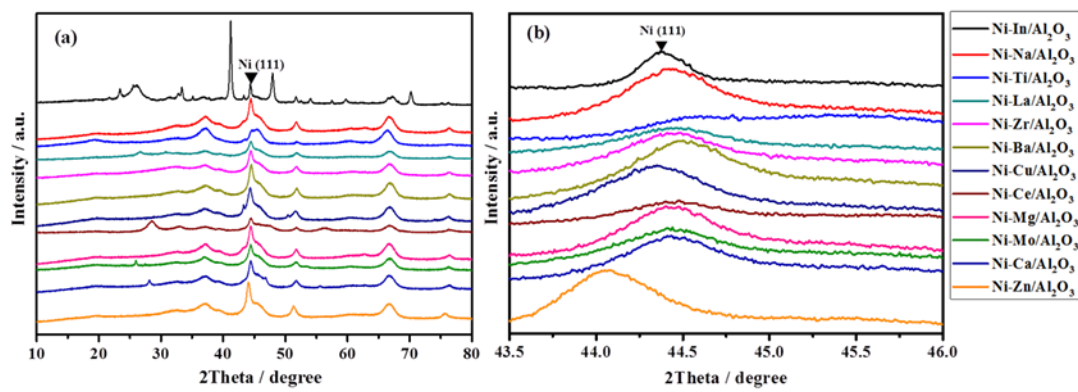


Figure S3

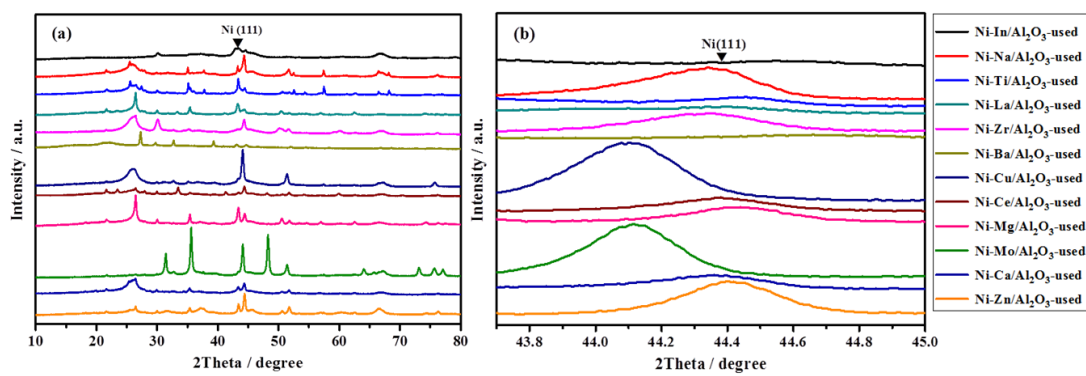


Figure S4

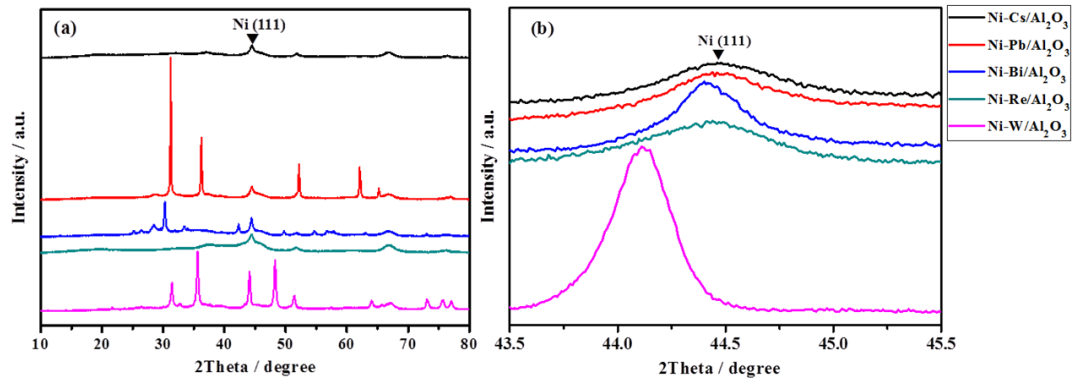


Figure S5

